

Optimizing microgrid designs towards net-zero emissions for smart cities: addressing energy disparities and access issues in Northern and North-eastern India

Albert Paul Arunkumar, Selvakumar Kuppusamy

Department of Electrical and Electronics Engineering, College of Engineering and Technology,
SRM Institute of Science and Technology, Kattankulathur, Chennai, India

Article Info

Article history:

Received Jul 11, 2024

Revised Sep 16, 2024

Accepted Oct 23, 2024

Keywords:

Energy access

Microgrids

Net-zero emissions

PSO

Smart cities

Sustainable development goals

ABSTRACT

Providing affordable and clean energy is a significant sub-sector of the Smart Cities Mission proposed by India. This research investigates the development of optimal microgrid designs for smart cities in northern and north-eastern India to address regional energy disparities and access issues. In the northern zone, characterized by uneven urban-rural infrastructure and high-power demand, microgrids offer localized, reliable solutions that reduce dependency on centralized systems and enhance energy efficiency. In the north-eastern zone, where geographical isolation and underdeveloped infrastructure hinder energy access, microgrids provide decentralized power generation and distribution, improving access in remote areas. The proposed microgrid designs aim to enhance energy reliability, efficiency, and accessibility by integrating renewable energy sources. The proposed system is analyzed for technical and economic feasibility based on critical factors such as cost of energy (COE), loss of power supply probability (LPSP), and the renewable fraction (RF). The renowned particle swarm optimization (PSO) algorithm is used to optimize the system size to achieve better performance in terms of technical and economic aspects. A proper energy management technique ensures the energy balance between the demand side and the distributed energy sources. A typical 24-hour household load profile is used for the optimization.

This is an open access article under the [CC BY-SA](#) license.



Corresponding Author:

Selvakumar Kuppusamy

Department of Electrical and Electronics Engineering, College of Engineering and Technology

SRM Institute of Science and Technology

Kattankulathur, Chennai, Tamil Nadu-603203, India

Email: selvakuk@srmist.edu.in, selvakse@gmail.com

1. INTRODUCTION

Due to rapid urbanization in recent decades, there is a need to develop a sustainable nature in the urban areas of a developing country like India which may provide very significant outcomes both in environmental and economic aspects. According to the United Nations Human Settlement Programme (UN-Habitat) [1], India's Smart Cities Mission (SCM) has three pillars: live-ability, economic-ability, and sustainability. When mapped (refer to Table 1) with the targets of Sustainable Development Goals (SDGs), these three pillars are found to be aligned with a total of 15 SDGs out of all 17 SDGs. On the other hand, in the eastern and north-eastern zones, energy access remains a critical challenge influenced by various factors. The eastern zone, comprising Bihar, Odisha, Sikkim, and Jharkhand, grapples with significant infrastructure deficiencies, including inadequate power generation, poor transmission, and distribution networks, leading to

frequent power outages and unreliable electricity supply. Rural areas in these states often face inconsistent power supply and high costs due to the uneven distribution of infrastructure. Similarly, the north-eastern states - Assam, Meghalaya, Arunachal Pradesh, Manipur, Nagaland, Mizoram, and Tripura experience challenges due to their remote locations and hilly terrain, which complicate grid extension and infrastructure development. Connectivity issues force many regions to rely on costly and less sustainable energy sources, resulting in limited and unreliable energy access. While policies are advancing energy access, significant improvements are needed to address the underlying infrastructure and economic barriers effectively. Taking this into account, the research proposes optimal-sized hybrid microgrid models for the cities selected to be upgraded as smart cities in the eastern and north-eastern zones by India's SCM.

Table 1. Mapping of SCM goals to 17 SDGs

SCM Goals	Sub-sector	SDGs Satisfied																
		1	2	3	4	5	6	7	8	9	10	11	12	13	14	15	16	17
Sustainability	Environments						✓		✓			✓	✓					
	Green Spaces and Buildings						✓					✓	✓			✓		
	Urban Resilience	✓										✓		✓				
	Energy Consumption							✓				✓	✓					
Liveability	Education		✓	✓	✓													
	Health	✓		✓					✓								✓	
	Housing & Shelter	✓				✓						✓						
	Slum upgradation	✓				✓						✓						
	Water supply	✓					✓			✓		✓						
	Sewerage and drainage	✓					✓					✓	✓					
	Solid waste management										✓	✓	✓				✓	
	Smart Roads			✓						✓		✓						
	NMT			✓								✓						
	Public transport	✓								✓		✓			✓		✓	
	Governance & ICT	✓								✓		✓		✓			✓	✓
	Recreation				✓		✓					✓				✓		
	Energy-related infrastructure	✓						✓				✓						
	Enhancement of Revenue sources						✓					✓					✓	✓
Economic ability	ICT-based	✓							✓								✓	✓
	Economic Opportunities				✓				✓	✓								
	Tourism economic opportunities								✓				✓				✓	

Smart grids are the future of electrical grids [2], and microgrids (MG) are the critical constituents of a smart grid [3]. MGs are small autonomous grids with distributed energy resources supplying controllable loads with energy storage systems for backup [4]. Such MGs can be operated in two modes: grid-connected (GC) and islanded mode (IM) [5]. When a MG suffices its needs from its resources without getting a backup from the utility grid, it operates in IM and vice versa. As the work focuses on satisfying the typical community loads, there is a need to consider a hybrid MG architecture, i.e., a MG with both alternating current (AC) and direct current (DC) feeders [6]. Also, this reduces the need for more power electronic conversion devices [7]. Therefore, hybrid MG architecture [8] is the chosen for this analysis. India is already focusing to increase its renewable capacity to 500 GW by the end of 2030 [9]. The major focus is on solar and wind resources. Therefore, these resources are considered. The intermittent nature of renewable energy sources mandates a power backup [10]. In case of IM operation, there will be no grid backup and a remote conventional power generation [11] resource is needed. Diesel generators (DiG) are the best remote generating systems considering this research. Therefore, the general hybrid microgrid (HM) system considered for optimization consists solar PV (SPV), wind turbines (WT), battery energy storage systems (BESS), DiG and loads along with necessary power electronic devices.

The planning of MGs includes several cost factors [12] such as capital cost, operation and maintenance (O&M) cost and replacement costs as the planning is done for a period of 25 years. The DiG involves certain parameters and constraints [13]. The primary objective is to design a system which meets loads with very less costs and high renewable penetration. A renowned optimization technique particle swarm optimization (PSO) [14] is used for optimization. To evaluate the optimal nature and feasibility, the parameters such as cost of energy (COE), loss of power supply probability (LPSP), and renewable fraction (RF) are considered. Literature review is shown in Table 2. In [15] the authors proposed a GC MG in Beijing

to optimize NPC and COE. A hybrid MG was designed by Abdin *et al.* [16] for IM operation in Beijing and a GC PV MG is enunciated in [17] for residential community. A HM model was analyzed for its feasibility in GC and IM operation by Das *et al.* [18]. A PV and biogas MG model is analyzed for various economic conditions by Kasaeian *et al.* [19] for Golshan city. Another PV-based GC MG is proposed in [20] for China. For rural electrification, authors in [21] proposed a GC model for Doddapalli, Andhra Pradesh. All these literatures used HOMER for optimization. A case study was carried out in Perth city by Essayeh *et al.* [22] using mixed integer non-linear programming. Taking only the NPC as objective, the author proposed a HM for Saint Martin Island [23]. Using SMO algorithm, a HM is proposed for SCM in Tamil Nadu by authors in [24].

The major research contributions of the article are listed below:

- Optimal HM models for all 16 cities in the eastern and north-eastern electrical zones are proposed using the optimized results of PSO.
- The technical and economic feasibility of the proposed models are analyzed and the best model with less COE, LPSP, and high RF are chosen to be the best optimal design for each city.
- The modelling includes all the cost elements to ensure the proper economic feasibility analysis.
- As the proposed MG system majorly uses renewable energy to generate power and the renewable fraction is taken into account, there will be a significant reduction in the total carbon footprint.

The rest of the article is organized as follows: Section 2 explains the mathematical modeling of the components of the hybrid microgrid system (HMGS). The adapted energy management strategy is elaborated in section 3. Section 4 enunciates the optimization technique used, whereas constraints and parameters related to the operation are presented in section 5. Section 6 concludes the article with the results and discussion.

Table 2. Literature review

Lit	Location	Microgrid model	Optimization	Parameters/goals
[15]	Beijing, China	WE+BESS+Grid	HOMER	LCOE & NPC
[16]	Bandar Abbas	PV+WE+Grid	HOMER	LCOE, NPC, & H ₂
[17]	Beijing, China	PV+Grid	HOMER	LCOE & NPC
[18]	Rajshahi	PV+DiG+BESS+Grid	HOMER	LCOE, NPC, & RF
[19]	Golshan	PV+DiG+Biogas+Grid	HOMER	LCOE, NPC, & RF
[20]	China	PV+DiG+Grid	HOMER	LCOE & NPC
[21]	Doddapalli	PV+WE+DiG+BESS+Grid	HOMER	LCOE, NPC, & RF
[22]	Perth city	PV+Grid	MINLP	LCOE & NPC
[23]	Bangladesh	PV+WE+Bio+Ecowave+BESS	HOMER	NPC
[24]	Tamilnadu	PV+WE+DiG+BESS	Spider monkey optimization (SMO)	LCOE, NPC, & RF

2. MATHEMATICAL MODELING OF THE HMGS COMPONENTS

This section presents the mathematical modeling of the HMGS components. The hybrid microgrid system consists of solar PVs, wind energy (WE) system, BESS, inverter, and diesel generator. The mathematical modelling of each component is elaborated with its associated parameters.

2.1. Modelling of solar PV (SPV)

The power output of the SPV system is calculated using the following mathematical expression as in (1).

$$P_{SPV}^{op} = P_{SPV}^n X \frac{G_{SPV}}{G_{SPVr}^{STC}} X [1 + \beta_{SPV}^t (T_{SPV}^{amb} + (0.0256 X G_{SPV}) - T_{SPV}^{STC})] \quad (1)$$

Where P_{SPV}^{op} is SPV output power, P_{SPV}^n is the SPV's rated power under reference conditions, G_{SPV} is the irradiation from the sun (W/m^2). The irradiation at standard test conditions (STC) is represented by G_{SPVr}^{STC} [$G_{SPVr}^{STC}=1000 W/m^2$] and T_{SPV}^{STC} represents the cell temperature ($^{\circ}C$) of SPV at STC. The ambient temperature of the SPV cell is represented by T_{SPV}^{amb} [$T_{PV}^a=250^{\circ}C$] and the β_{SPV}^t is $(-3.7 \times 10^{-3} (1/^{\circ}C))$ which is the temperature coefficient.

2.1.1. Modelling of wind energy (WE) system

The recorded wind speeds are converted in terms of equivalent wind turbine height values to calculate the power generated.

$$\frac{v_w^{hh}}{v_w^{ref}} = \left(\frac{h_r^{hub}}{h_r^{ref}} \right)^{\alpha} \quad (2)$$

V_w^{hh} (m/s) and V_w^{ref} (m/s) is the wind velocity at WT hub (h_{WT}^{hub}) and reference height (h_T^{ref}) respectively. The hub and reference height of a WT are represented by h_{WT}^{hub} (m) and h_{WT}^{ref} (m), respectively. α is the Hellmann exponent. The WT rated velocity is V_r (m/s), $V_{cut-out}$ (m/s) and V_{cut-in} (m/s) denote the WT cut-out and cut-in velocity respectively. The WT power output can be defined as (3). Where, P_{WT} is the actual power generated by WT, P_{WT}^r (kW) is the WT rated power and V_w (m/s) is the wind velocity.

$$P_{WT} = \begin{cases} 0, & \text{if } V_w < V_{cut-in}, V_w > V_{cut-out} \\ \frac{P_{WT}^r}{V_r^3 - V_{cut-in}^3} [V^3 - V_{cut-in}^3] & \text{if } V_{cut-in} \leq V_w \leq V_r \\ P_{WT}^r & \text{if } V_r \leq V_w < V_{cut-out} \end{cases} \quad (3)$$

2.3. Modelling of BESS and inverter

Instead of traditional BESS modeling, the AuD and the load required are incorporated to calculate the capacity of the battery. Where B_c is the battery capacity, L_{req} is required load, N_{AD} is the number of AuD, D_b^{dod} is the battery's depth of discharge (80%), η_i and η_b represents the efficiencies of the inverter (95%) and battery (85%). The highest SOC (SOC_b^{max}) and lowest SOC (SOC_b^{min}) of the battery are used to determine its present SOC_b^t . The energy excess or deficit of the battery storage system can be explained as (4) and (5).

$$B_c = \frac{L_{req} \cdot N_{AD}}{D_b^{dod} \cdot \eta_b \cdot \eta_i} \quad (4)$$

$$P_b^t = (P_{SPV}^t + P_{WE}^t) - \frac{L_{req}^t}{\eta_i} \quad (5)$$

$P_b^t < 0$ and $P_b^t > 0$ represents the shortfall and excess of battery power needed to match the load demand for hour t , respectively. P_{SPV}^t represents the SPV power produced in hour t . P_{WE}^t represents the wind energy produced in hour t . The customer load pattern for hour t is L_{req}^t where, η_i denotes inverter efficiency. SOC_b^t and $SOC_b^{(t-1)}$ represents the SOC of the battery during hour t and the previous hour ($t-1$) respectively where the charging and discharging power of the battery at the present hour t is represented by P_b^t and $-P_b^t$ respectively.

$$SOC_b^t = SOC_b^{(t-1)}(1 - \delta^b) + (-P_b^t + \eta_b) \quad (6)$$

$$\eta_i = \frac{\left(\frac{L_{out}}{L_n}\right)}{\left(\frac{L_{out}}{L_n}\right) + \left(1 - 99\left(\frac{1}{\eta_p} - \frac{1}{\eta_q} - 9\right)^2\right) + \left(\frac{1}{\eta_q} - 1 - 99\left(\frac{1}{\eta_p} - \frac{1}{\eta_q} - 9\right)^2 - 1\right)\left(\frac{L_{out}}{L_n}\right)^2} \quad (7)$$

The inverter efficiency is calculated by (7). δ^b and η_b denotes the self-discharge rate and battery efficiency respectively. Where η_p and η_q denotes the inverter's efficiency at 10% and 100% of its nominal power, respectively.

2.4. Modelling of diesel generator

The efficiency of the diesel generator is calculated by evaluating the power produced to the rate of fuel consumption.

$$F^t = aP_{DiG}^t + bP_{DiG}^r \quad (8)$$

P_{diesel}^t represents the diesel power generated in (kW) by consuming fuel per hour (L/hour) denoted by F^t at time t . P_{diesel}^r is rated nominal power (kW) of the diesel plant. The fuel usage coefficients (constants) are represented by the values a and b , which are nearly equivalent to 0.246 and 0.08415, respectively.

3. SMART ENERGY MANAGEMENT STRATEGY AND PARAMETERS FOR ANALYSIS

To facilitate the optimal use of resources and to ensure the energy demand balance the following smart energy management strategy is applied. The strategy is mapped as follows:

- The renewable energy resources (RERs) (PV+WT) generate sufficient energy and meets the load if $L_{req}^t > \frac{L_{req}^t}{\eta_i}$. Then, the excess energy is used for charging the battery until $SOC_b^t = SOC_b^{max}$.
- The (RERs) are unable to generate enough energy to meet the load, and $SOC_b^t > SOC_b^{min}$. Therefore, the battery bank's power will serve as the main backup.
- The RERs can meet customer demand during hour t if $L_{req}^t = \frac{L_{req}^t}{\eta_i}$; but, if $DOD_b^t \geq DOD_b^{max}$ at that time, PV and WT are unable to replenish the battery bank.
- The battery bank is empty ($DOD_b^t = DOD_b^{max}$) and the RERs are not able to meet the load ($L_{req}^t < \frac{L_{req}^t}{\eta_i}$).

The DG acts as a secondary backup source to meet load and replenish the battery bank.

The parameters and operational constraints considered are explained further in the feasibility analysis of the system. The three major parameters of consideration are COE, LPSP, and RF.

3.1. Cost of energy

COE is one of the most popular and extensively used indicators of the financial feasibility of hybrid energy systems. It is the ratio of the total NPC (\$) to the annual load (kWh). The total NPC includes all capital costs, O&M expenses, and replacement prices. The hourly customer load usage is denoted by P_{load} (h).

3.1.1. Capital cost

The price of buying the components of an HM shown in Figure 1, such as the DiG, SPV panels, WT, and battery, constitutes the capital cost. The total anticipated cost of all the MG system's components makes up the system's capital cost. The capital cost is defined as (9).

$$C^{cap} = \{x^{DiG} C^{DiG} R^{DiG} + x^{SPV} C^{SPV} R^{SPV} + x^{WE} C^{WE} R^{WE} + x^b C^b R^b + x^i C^i R^i\} \quad (9)$$

Where x^{DiG} , x^{SPV} , x^{WE} , x^b , x^i are the ratings of diesel generator, SPV, WT, battery, and inverter respectively and C^{DiG} , C^b , and C^i are the costs per kW for DiGs, battery, and inverter respectively. C^{SPV} and C^{WE} are plant installation costs per kW for SPV and WT respectively. The ON/OFF status of each unit is denoted by the decision variables in HM system.

$$\begin{aligned} R_{DiG} &= \begin{cases} 1 & \text{Diesel Generator is Up} \\ 0 & \text{Diesel Generator is Down} \end{cases}, R_{SPV} = \begin{cases} 1 & \text{Solar PV System is Up} \\ 0 & \text{Solar PV System is Down} \end{cases} \\ R_{WT} &= \begin{cases} 1 & \text{Wind Power is Up} \\ 0 & \text{Wind Power is Down} \end{cases}, R_b = \begin{cases} 1 & \text{Battery is Up} \\ 0 & \text{Battery is Down} \end{cases}, R_i = \begin{cases} 1 & \text{Inverter is Up} \\ 0 & \text{Inverter is Down} \end{cases} \quad (10) \end{aligned}$$

Where R_{DiG} , R_{SPV} , R_{WT} , R_b , and R_i are decision variables associated with DiGs, SPV, WT, batteries, and inverters respectively.

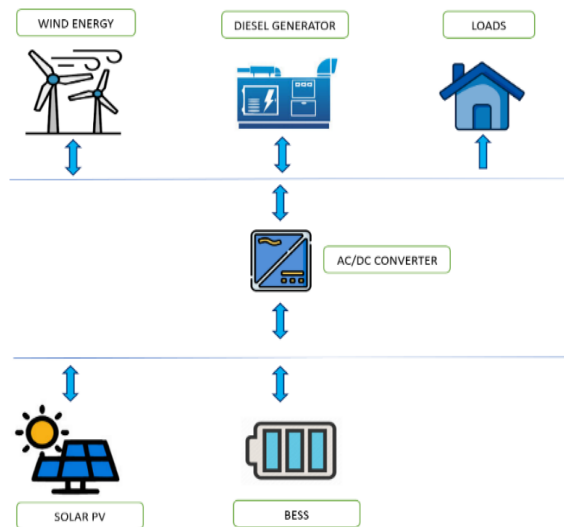


Figure 1. The general architecture of the considered HMGS

3.1.2. Operation and maintenance costs

O&M costs vary and are influenced by interest rates and inflation. For the sake of this study, the inflation and interest rates of the MG system components are set at 5% and 13%, respectively.

$$C^{om} = \begin{cases} \left[\frac{(1+d)}{(s-d)} \right] \left[1 - \left(\frac{1+d}{1+s} \right)^{CLT} \right] \{ C_{om}^{DiG} R^{DiG} + C_{om}^{SPV} R^{SPV} + C_{om}^{WE} R^{WE} + C_{om}^b R^b + C_{om}^i R^i \}, & \text{for } (s \neq d) \\ \{ C_{om}^{DiG} R^{DiG} + C_{om}^{SPV} R^{SPV} + C_{om}^{WE} R^{WE} + C_{om}^b R^b + C_{om}^i R^i \} \times CLT, & \text{for } (s = d) \end{cases} \quad (11)$$

d is inflation rate for component replacement, and s is real interest rate. The component life time in a year is denoted by CLT . $C_{o\&m}^{DiG}$, $C_{o\&m}^{SPV}$, $C_{o\&m}^{WT}$, $C_{o\&m}^{BAT}$, and $C_{o\&m}^{inv}$ represents O&M costs for diesel generator, SPV, WT, battery, and inverter, respectively.

3.1.3. Replacement costs

The cost of replacing the MG system's component parts is considered at each step of the system's lifespan. Consequently, the project's current approximation is evaluated for all component replacement costs. The present cost of replacing a MG system can be expressed as (12).

$$C^{re} = \left(\frac{1+d}{1+s} \right)^{CLT} \left\{ C_{re}^{DiG} C_{unit}^{DiG} R^{DiG} + C_{re}^{SPV} C_{unit}^{SPV} R^{SPV} + C_{re}^{WE} C_{unit}^{WE} R^{WE} + C_{re}^b C_{unit}^b R^b + C_{re}^i C_{unit}^i R^i \right\} \quad (12)$$

C_{unit}^{DiG} is the component cost of the diesel generator unit. Similarly, C_{unit}^{SPV} , C_{unit}^{WE} , C_{unit}^b , C_{unit}^i denotes the unit component costs of the SPV generation, WT, battery, and the inverter respectively. C_{re}^{DiG} , C_{re}^{SPV} , C_{re}^{WE} , C_{re}^b , and C_{re}^i represents the replacement cost of diesel generator, SPV, WT, battery, and the inverter respectively.

3.2. Loss of power supply probability (LPSP)

The HM system's reliability is assessed using the LPSP. The chance that the power supply is able to meet demand due to a lack of energy from renewable sources or technical issues is indicated by the LPSP which is expressed by (13).

$$LPSP = \frac{\sum_{t=1}^{8760} (L_{req}^t - P_{SPV}^t - P_{WE}^t + P_b^{min,t})}{\sum_{t=1}^{8760} L_{req}^t} \quad (13)$$

At time t , the power generated by SPV, WT, and diesel generator can be denoted by P_{SPV}^t , P_{WE}^t , and P_{DiG}^t respectively. Where the load at t is represented by L_{req}^t . P_b^{min} denotes the battery minimum storage capacity. The literature indicates that the LPSP value needs to be less than 5%. A challenging scenario is used to perform the reliability assessment in this study, when $L_{req}^t > P_{gen}^t$, where P_{gen}^t represents the total power generated by the whole system during time t .

3.3. Renewable fraction (RF)

In optimization programming, RF is a threshold used to compare the energy produced by a diesel power generator with a renewable power generator. When the renewable component is zero, the hybrid MG system fully relies on a diesel generator to provide its electrical demands. The (14) can be used to describe it. The range of the RF is 0 to 1. Whereas 1 denotes complete reliance on renewable energy sources and 0 denotes no use of renewable energy.

$$RF(\%) = \left(1 - \frac{\sum_{t=1}^{8760} P_{diesel}^t}{\sum_{t=1}^{8760} (P_{PV}^t + P_{WT}^t)} \right) \times 100 \quad (14)$$

4. OPTIMIZATION TECHNIQUE AND METHODOLOGY

Three criteria (RF, COE, and LPSP) are taken into account for choosing an economically viable MG design with the ideal size. The economics and power supply dependability are of major emphasis. Therefore, the two variables COE and LPSP are selected as the goals. The multi-objective problem is reduced to a single objective for computational simplicity. Since both goals are equally important, they are each given equal weights of 0.5. The fitness function [25] can be written as (15). The constraints define as $ming_i(x) \geq 0$ for $i \in \{1, \dots, l\}$.

$$fitness = \min \left\{ \sum_{i=1}^k w_i \frac{f_i(x)}{f_i^{max}} \right\} \text{ with } w_i \geq 0 \text{ and } \sum_{i=1}^k w_i = 1 \quad (15)$$

x represents the vector of decision variables and W_i stands for the weight equivalent significance of each objective, K denotes the weight of the objective and f is the objective function whose upper bound is denoted by f_i^{max} . Due to the high converging nature of PSO, it is selected for optimization. For a defined fitness function, the fitness of each particle is evaluated first. Followed by the velocity and position of each particle is updated to determine the individual and global best fitness position.

The swarm position of each particle is updated using (16).

$$x_{k+1}^i = x_k^i + V_{k+1}^i \quad (16)$$

$$V_{k+1}^i = K \times [V_k^j + c_1 r_1 (P_k^i - x_k^i) + c_2 r_2 (P_k^g - x_k^i)] \quad (17)$$

$$k = \frac{2}{2 - \phi - \sqrt{\phi^2 - 4\phi}} \quad (18)$$

Where, x and v represents the position and velocity of particle in the iteration k , $c_1 r_1 (P_k^i - x_k^i)$ – individual component, and $c_2 r_2 (P_k^g - x_k^i)$ – Social Component. The planning concerns discussed in this article are addressed by the four choice variables - the no. of SPV panels, WT, diesel generators, and AuD.

Considering the region where the MG is being built, the following restrictions should be applied to the decision variables.

$$0 \leq N_{SPV} \leq N_{SPV}^{max}, 0 \leq N_{WE} \leq N_{WE}^{max}, 0 \leq N_{AuD} \leq N_{AuD}^{max}, 0 \leq N_{DiG} \leq N_{DiG}^{max} \quad (19)$$

N_{SPV} and N_{WE} are no. of SPV panels and WT respectively, N_{AuD} and N_{DiG} are number of diesel generators, AuD, N_{SPV}^{max} , N_{WE}^{max} , N_{AuD}^{max} , and N_{DiG}^{max} are maximum no. of SPV panels and WT (AuD) and diesel generator respectively.

5. SIMULATION AND DISCUSSION OF THE RESULTS

The typical 24-hour load profile shown in Figure 2 is considered for the simulation. The wind speed, irradiance, and cell temperature are obtained from the NASA power data access viewer website for the selected locations. A sample of data obtained is shown for two cities in Figure 3 along with a sample pareto curve. To attain convergence, 100 iterations using 100 particles each time were carried out for every simulation.

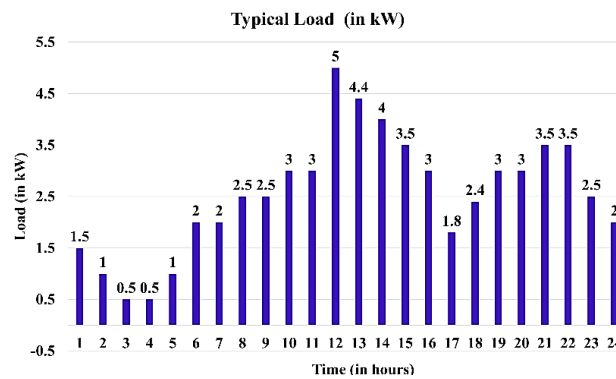


Figure 2. Typical 24-hour load profile considered for optimization

5.1. Eastern region

The simulation results obtained for the nine cities in the eastern electrical zone is discussed in this section. Figure 4(a) shows the optimal size of the HMGS obtained whereas, the LPSP, COE, RF, and AuD are shown in Figure 4(b). Among the 9 cities of the eastern region, Biharsharif achieves very less COE (2.2094 \$/kWh), making it the most economic model, whereas, Muzaffarpur exhibits a very less LPSP

(0.01435) and is the most reliable model in the eastern zone. Also, Muzaffarpur exhibits a higher RF of 57.875%. Also, three cities: Bhagalpur, Biharsharif, and Muzaffarpur exhibit a good performance for number of AuD with a total of 8 days. Taking all parameters into account, the model developed for Muzaffarpur, exhibits best optimal performance.

5.2. North-eastern region

The optimal size and value of parameters evaluated for the HMGS for the North-Eastern zone is shown in Figures 5(a) and 5(b) respectively (see in Appendix). Kohima has a very good economic model with a COE of 2.2364 \$/kWh and Pasighat exhibits a very less LPSP of 0.2575 which makes it the reliable model in the north-eastern region. On account of RF, Agartala model founds to utilize renewable energy a lot for the energy production with a value of 65.85% RF. Also, Agartala & Imphal is found to have a high number of AuD (9 days).

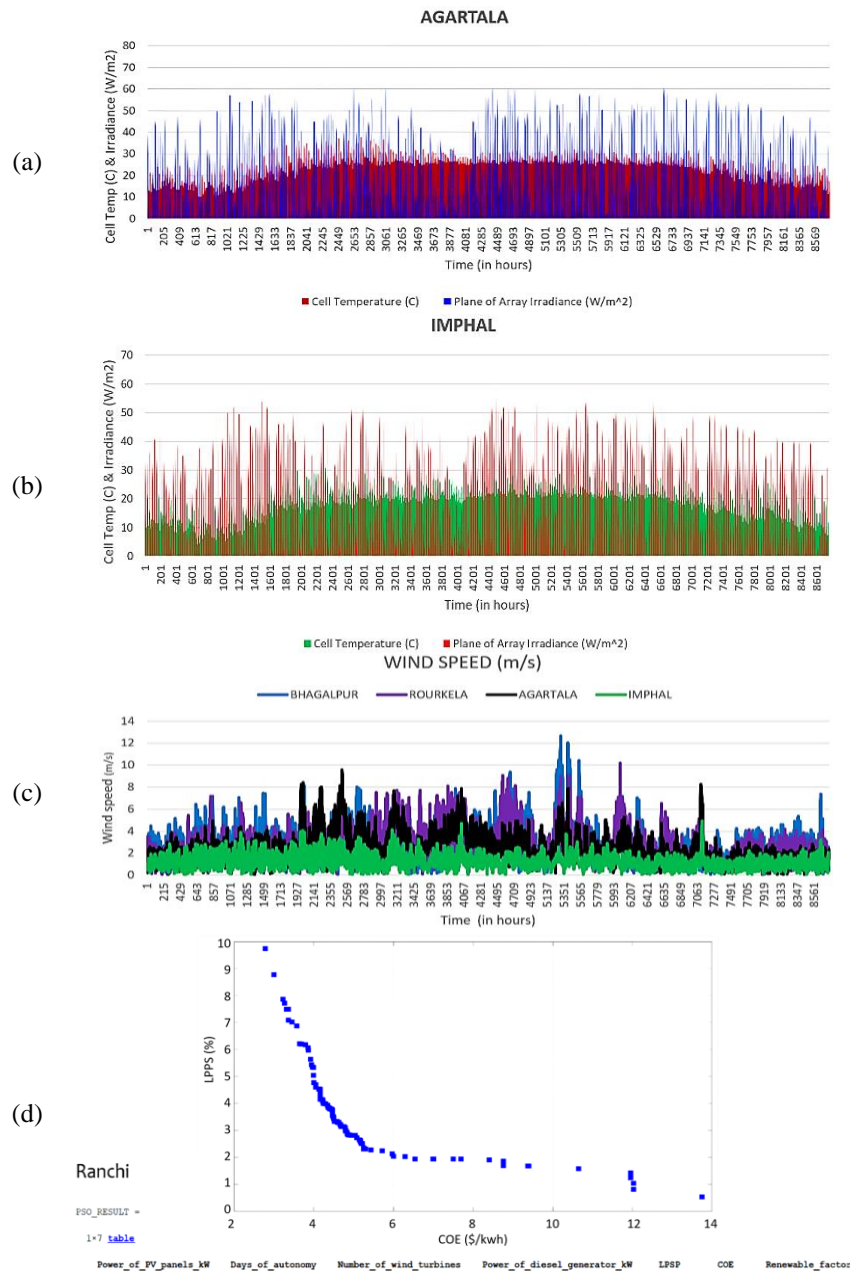


Figure 3. Weather characteristics (hourly irradiance and cell temperature data) obtained for (a) Agartala, (b) Imphal, (c) hourly wind speed data, and (d) Pareto curve and the simulation result for Ranchi using PSO

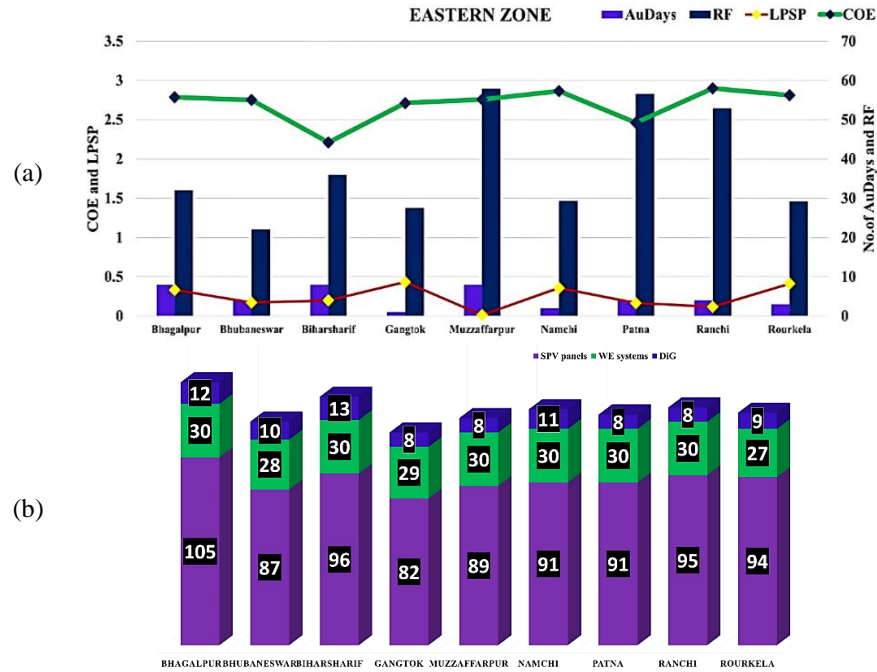


Figure 4. The simulation results for Eastern zone cities: (a) optimal size and (b) optimized parameters

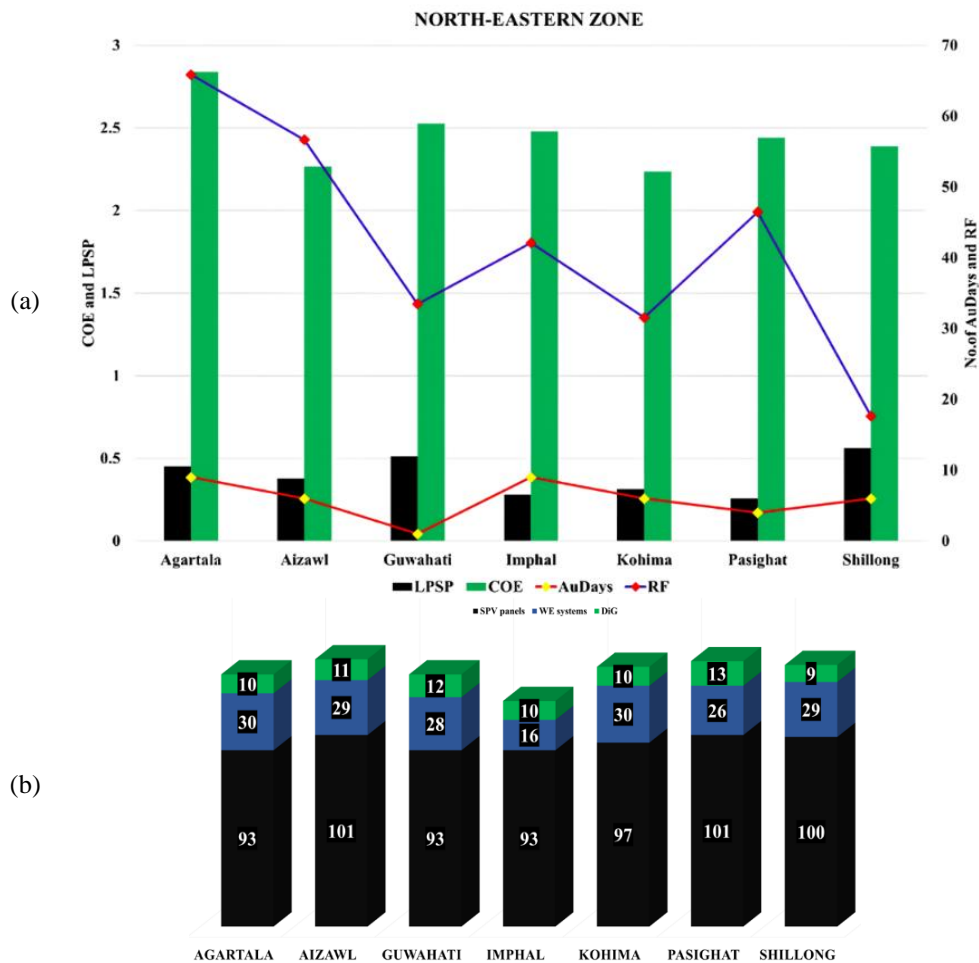


Figure 5. The simulation results for North-Eastern zone cities: (a) optimal size and (b) optimized parameters

6. CONCLUSION AND FUTURE SCOPE

The proposed hybrid microgrid system (HMGS) model, enhanced with a smart energy management system (SEMS), has been optimized to address energy access issues and disparities in the smart cities designated in India's eastern and northeastern zones. The optimization process determined the ideal system sizes, ensuring a comprehensive economic model that accounts for all cost elements, including inflation. This model aims to mitigate regional energy disparities by improving energy reliability and accessibility. In the eastern zone, the MG model for Muzaffarpur excels in terms of all performance metrics, addressing the region's infrastructure deficiencies and providing a reliable energy solution. In the northeastern zone, Agartala is identified as the optimal model due to its high renewable fraction and excellent autonomy days, which effectively tackle the challenges of geographical isolation and intermittent power supply. The integration of renewable energy sources and efficient management strategies in these models significantly enhances energy access in areas that face significant infrastructure and economic constraints. Future work could include sensitivity analysis to further refine these models and evaluate their robustness under varying conditions, ensuring continued improvement in addressing energy access challenges.





REFERENCES

- [1] N. M. Kumar, S. Goel, and P. K. Mallick, "Smart cities in India: Features, policies, current status, and challenges," in *2018 Technologies for Smart-City Energy Security and Power (ICSESP)*, IEEE, Mar. 2018, pp. 1–4, doi: 10.1109/ICSESP.2018.8376669.
- [2] L. Quitzow and F. Rohde, "Imagining the smart city through smart grids? Urban energy futures between technological experimentation and the imagined low-carbon city," *Urban Studies*, vol. 59, no. 2, pp. 341–359, Feb. 2022, doi: 10.1177/00420980211005946.
- [3] S. S. Rangarajan *et al.*, "DC microgrids: A propitious smart grid paradigm for smart cities," *Smart Cities*, vol. 6, no. 4, pp. 1690–1718, Jul. 2023, doi: 10.3390/smartcities6040079.
- [4] A. P. Arunkumar, S. Kuppusamy, S. Muthusamy, S. Pandiyan, H. Panchal, and P. Nagaiyan, "An extensive review on energy management system for microgrids," *Energy Sources, Part A: Recovery, Utilization and Environmental Effects*, vol. 44, no. 2, pp. 4203–4228, 2022, doi: 10.1080/15567036.2022.2075059.
- [5] A. Hirsch, Y. Parag, and J. Guerrero, "Microgrids: A review of technologies, key drivers, and outstanding issues," *Renewable and Sustainable Energy Reviews*, vol. 90, no. March, pp. 402–411, 2018, doi: 10.1016/j.rser.2018.03.040.
- [6] J. Singh, S. Prakash Singh, K. S. Verma, A. Iqbal, and B. Kumar, "Recent control techniques and management of AC microgrids: A critical review on issues, strategies, and future trends," *International Transactions on Electrical Energy Systems*, no. July, pp. 1–39, 2021, doi: 10.1002/2050-7038.13035.
- [7] M. S. Mahmoud, M. S. U. Rahman, and F. M. A. L. Sunni, "Review of microgrid architectures - a system of systems perspective," *IET Renewable Power Generation*, vol. 9, no. 8, pp. 1064–1078, 2015, doi: 10.1049/iet-rpg.2014.0171.
- [8] M. S. Bin Arif and M. A. Hasan, "Microgrid architecture, control, and operation," in *Hybrid-Renewable Energy Systems in Microgrids*, Elsevier, 2018, pp. 23–37, doi: 10.1016/B978-0-08-102493-5.00002-9.
- [9] A. Mathur and S. Singh, "Status of India's renewable energy commitments for the Paris agreement," in *2019 International Conference on Power Generation Systems and Renewable Energy Technologies (PGSRET)*, IEEE, Aug. 2019, pp. 1–5, doi: 10.1109/PGSRET.2019.8882701.
- [10] P. Nagapurkar and J. D. Smith, "Techno-economic optimization and social costs assessment of microgrid-conventional grid integration using genetic algorithm and artificial neural networks: A case study for two US cities," *Journal of Cleaner Production*, vol. 229, pp. 552–569, Aug. 2019, doi: 10.1016/j.jclepro.2019.05.005.
- [11] J. D. Lara, D. E. Olivares, and C. A. Cañizares, "Robust energy management of isolated microgrids," *IEEE Systems Journal*, vol. 13, no. 1, pp. 680–691, Mar. 2019, doi: 10.1109/JSYST.2018.2828838.
- [12] P. Nagapurkar and J. D. Smith, "Techno-economic optimization and environmental life cycle assessment (LCA) of microgrids located in the US using genetic algorithm," *Energy Conversion and Management*, vol. 181, pp. 272–291, Feb. 2019, doi: 10.1016/j.enconman.2018.11.072.
- [13] F. Jabari, H. Arasteh, A. Sheikhi-Fini, and B. Mohammadi-Ivatloo, "Optimization of a tidal-battery-diesel driven energy-efficient standalone microgrid considering the load-curve flattening program," *International Transactions on Electrical Energy Systems*, vol. 31, no. 9, Sep. 2021, doi: 10.1002/2050-7038.12993.
- [14] H.-T. Yang, C.-T. Yang, C.-C. Tsai, G.-J. Chen, and S.-Y. Chen, "Improved PSO based home energy management systems integrated with demand response in a smart grid," in *2015 IEEE Congress on Evolutionary Computation (CEC)*, IEEE, May 2015, pp. 275–282, doi: 10.1109/CEC.2015.7256902.
- [15] M. Gharibi and A. Askarzadeh, "Technical and economical bi-objective design of a grid-connected photovoltaic/diesel generator/fuel cell energy system," *Sustainable Cities and Society*, vol. 50, p. 101575, Oct. 2019, doi: 10.1016/j.scs.2019.101575.
- [16] Z. Abdin and W. Mérida, "Hybrid energy systems for off-grid power supply and hydrogen production based on renewable energy: A techno-economic analysis," *Energy Conversion and Management*, vol. 196, pp. 1068–1079, Sep. 2019, doi: 10.1016/j.enconman.2019.06.068.
- [17] L. He, S. Zhang, Y. Chen, L. Ren, and J. Li, "Techno-economic potential of a renewable energy-based microgrid system for a sustainable large-scale residential community in Beijing, China," *Renewable and Sustainable Energy Reviews*, vol. 93, pp. 631–641, Oct. 2018, doi: 10.1016/j.rser.2018.05.053.
- [18] B. K. Das, M. A. Alotaibi, P. Das, M. S. Islam, S. K. Das, and M. A. Hossain, "Feasibility and techno-economic analysis of stand-alone and grid-connected PV/Wind/Diesel/Batt hybrid energy system: A case study," *Energy Strategy Reviews*, vol. 37, p. 100673, Sep. 2021, doi: 10.1016/j.esr.2021.100673.
- [19] A. Kasaean, P. Rahdan, M. A. V. Rad, and W.-M. Yan, "Optimal design and technical analysis of a grid-connected hybrid photovoltaic/diesel/biogas under different economic conditions: A case study," *Energy Conversion and Management*, vol. 198, p. 111810, Oct. 2019, doi: 10.1016/j.enconman.2019.111810.





- [20] C. Li *et al.*, “Techno-economic and environmental evaluation of grid-connected and off-grid hybrid intermittent power generation systems: A case study of a mild humid subtropical climate zone in China,” *Energy*, vol. 230, p. 120728, Sep. 2021, doi: 10.1016/j.energy.2021.120728.
- [21] N. C. Alluraiah and P. Vijayapriya, “Optimization, Design, and Feasibility Analysis of a Grid-Integrated Hybrid AC/DC Microgrid System for Rural Electrification,” *IEEE Access*, vol. 11, pp. 67013–67029, 2023, doi: 10.1109/ACCESS.2023.3291010.
- [22] C. Essayeh and T. Morstyn, “Optimal sizing for microgrids integrating distributed flexibility with the Perth West smart city as a case study,” *Applied Energy*, vol. 336, p. 120846, Apr. 2023, doi: 10.1016/j.apenergy.2023.120846.
- [23] M. Asaduz-Zaman, W. Ongsakul, and M. J. Hossain, “Microgrid Energy Management for Smart City Planning on Saint Martin’s Island in Bangladesh,” *Energies*, vol. 16, no. 10, p. 4088, May 2023, doi: 10.3390/en16104088.
- [24] T. S. Kumar and T. Venkatesan, “A Techno-Economic Optimal Evaluation and Feasibility Analysis of Hybrid Microgrid Electrification for Smart Cities in Tamil Nadu,” *Electric Power Components and Systems*, vol. 52, no. 11, pp. 1981–1997, Jul. 2024, doi: 10.1080/15325008.2023.2249883.
- [25] K. Selvakumar, R. Anuradha, and A. Paul Arunkumar, “Techno-economic assessment of a hybrid microgrid using PSO,” *Materials Today: Proceedings*, vol. 66, pp. 1131–1139, 2022, doi: 10.1016/j.matpr.2022.04.919.

BIOGRAPHIES OF AUTHORS



Albert Paul Arunkumar     received his bachelor’s degree in Electrical and Electronics Engineering and the master’s degree in Power Systems Engineering in 2017 and 2020 from Anna University, Chennai. Currently, he is pursuing a Ph.D., in Electrical Engineering at SRM University. His research interests include microgrids, renewable energy systems, energy management systems, and deregulated power systems. He can be contacted at email: aa7426@srmist.edu.in.



Selvakumar Kuppasamy     received his B.E. degree in Electrical and Electronics Engineering from Anna University, Chennai, India in the year 2010. He obtained his M.E degree in Power Systems in the year 2012 from K.S. Rangasamy College of Technology under Anna University, Chennai, India, and his Ph.D., in SRM Institute of Science and Technology, Kattankulathur, Chennai. He is currently working as an assistant professor in the Department of Electrical and Electronics Engineering, SRM Institute of Science and Technology, Chennai, India. He has published 75 research papers in international journals. He has presented 20 papers at international conferences. His research interests are generation scheduling, power system operation, power flow analysis, and soft computing techniques in microgrids. He is a life member of ISTE, MIE, IAENG, IACSIT, IRED, and member of IEEE. He can be contacted at email: selvakuk@srmist.edu.in or selvakse@gmail.com.